Lawrence Berkeley Laboratory

UNIVERSITY OF CALIFORNIA

Submitted to Magnetic Resonance in Medicine

Magnethohydrodynamics of Blood Flow

J.R. Keltner, M.S. Roos, P.R. Brakeman, and T.F. Budinger

May 1989

Donner Laboratory

Biology & Medicine Division

Prepared for the U.S. Department of Energy under Contract Number DE-AC03-76SF00098.

DISCLAIMER

Magnetohydrodynamics of Blood Flow

John R. Keltner, Mark S. Roos, Paul R. Brakeman, and Thomas F. Budinger

Donner Laboratory

Research Medicine and Radiation Biophysics Division

Lawrence Berkeley Laboratory

1 Cyclotron Road

Berkeley, CA 94720

Magnetohydrodynamics of Blood Flow

John R. Keltner

Lawrence Berkeley Laboratory, MS 55-121

1 Cyclotron Road

Berkeley, CA 94720

Abstract

The changes in hydrostatic pressure and electrical potentials across vessels in the human vasculature in the presence of a large static magnetic field are estimated to determine the feasibility of in vivo NMR spectroscopy at fields as high as 10 Tesla. A 10 Tesla magnetic field changes the vascular pressure in a model of the human vasculature by less than 0.2 percent. An exact solution to the magnetohydrodynamic equations describing a conducting fluid flowing transverse to a static magnetic field in a non-conducting, straight, circular tube is used. This solution is compared to an approximate solution that assumes no magnetic fields are induced in the fluid and that has led previous investigators to predict significant biological effects from static magnetic fields. Experimental results show the exact solution accurately predicts the magnetohydrodynamic slowing of 15 percent NaCl flowing transverse to 2.3 Tesla and 4.7 Tesla magnetic fields for fluxes below 0.5 l/min while the approximate solution predicts a much more retarded flow.

Introduction

Interest in performing in vivo NMR spectroscopy at fields as high as 10 Tesla has raised questions about the effects of large magnetic fields on the human body. This paper is concerned with changes in vascular pressure and electrical potentials across vessels at high magnetic fields. As early as 1937, Hartman predicted (1) and with Lazarus verified (2) that conducting fluids flowing transversely to a magnetic field develop induced currents resulting from the Lorentz force . The induced currents interacting with the transverse magnetic field produce body forces on the fluid resulting in an increase in pressure gradient in the direction of fluid flow. Hartman solved for the pressure gradient in non-conducting, square ducts with flow transverse to a magnetic field, and in 1962 Gold published an exact solution for circular tubes (3). In 1973, Vardanyan obtained an approximate solution for conducting liquids flowing in non-conducting, circular tubes with flow transverse to a magnetic field by assuming that no magnetic fields are induced in the fluid (4). In the first section, these two solutions are presented. In the following sections the exact solution and the approximate solution are compared with data obtained by Hartman and Lazarus for mercury and with the experimental data for saline. The exact solution predicts an increase in pressure gradient that agrees with the experimental results obtained by Hartman and Lazarus and with the results presented here. The approximate solution predicts a much larger increase in pressure gradient than observed in the mercury or saline magnetohydrodynamic experiments. This approximate solution has led previous authors to predict that 5 Tesla static magnetic fields reduce blood velocity in the aorta up to 10 percent (5, 6). In the final section of this paper, the exact solution is used to estimate the magnetohydrodynamic increase in vascular pressure and the induced electric potentials across vessels.

Statement of Problem

Assume a steady flow in a rigid circular tube. The only nonzero component of the velocity vector is the axial component, v_z. The Navier-Stokes equation of motion for a constant pressure gradient G in the presence of a transverse magnetic field is

$$G = \mu \vec{j} \times \vec{B} + \eta \nabla^2 v_z, \qquad [1]$$

where η is the viscosity and μ is the permeability. The $\mu \vec{j} \times \vec{B}$ term is the Lorentz force resulting from the interaction of the current $\vec{j}$ with the magnetic field $\vec{B}$. Using Ampere's law and a double cross product vector identity, the Lorentz force may be rewritten as

$$G = \frac{\mu}{4\pi}\left[(\vec{B} \cdot \nabla)\vec{B} - \frac{1}{2}\nabla(\vec{B} \cdot \vec{B})\right] + \eta \nabla^2 v_z, \qquad [2]$$

Using Faraday's law, Ampere's law, Ohm's law, and the transformation properties of electromagnetic fields, it is straightforward to derive the second equation of motion for the magnetic field in a fluid with conductivity σ:

$$(4\pi\sigma\mu) \nabla \times (\vec{v} \times \vec{B}) + \nabla^2 \vec{B} = 0. \qquad [3]$$

In both of these equations it is assumed that the velocity and magnetic field are divergenceless. The assumption that only v_z is nonzero and the above two equations of motion imply that only the axial component of the induced magnetic field B_I is nonzero. In cylindrical coordinates (r, θ, z) the magnetic field in the fluid is:

$$B_r(\theta) = B_o cos\theta, \qquad B_\theta(\theta) = -B_o sin\theta, \qquad B_z(r,\theta) = B_I(r,\theta), \qquad [4]$$

where B_o is the applied magnetic field.

Since B_z is the only nonzero component of the induced magnetic field, Ampere's law leads to the induced current in the fluid:

$$j_r = (\frac{1}{4\pi r})\frac{\partial B_z}{\partial \theta}, \quad [5]$$

$$j_\theta = -(\frac{1}{4\pi})\frac{\partial B_z}{\partial r}, \quad [6]$$

$$j_z = 0. \quad [7]$$

Ohms law yields the induced electric fields $\vec{E}$,

$$E_r = (\frac{1}{\sigma})j_r + \mu v_z B_\theta, \quad [8]$$

$$E_\theta = (\frac{1}{\sigma})j_\theta - \mu v_z B_r, \quad [9]$$

$$E_z = 0. \quad [10]$$

Exact Solution

In 1962, Gold published exact solutions for the velocity profile and the induced magnetic field for laminar fluid flow in a non-conducting, straight, circular tube transverse to a magnetic field. His results are summarized below. In cylindrical coordinates the solution for the velocity profile in a tube of radius R is

$$v_z(r,\theta) = -\frac{GR^2}{4\eta\alpha}\psi_1, \quad [11]$$

where

$$\psi_1 = \left[e^{-\alpha\beta\theta} \sum_{n=0}^{\infty} \epsilon_n \frac{I_n'(\alpha)}{I_n(\alpha)} I_n(\alpha\beta) cosn\theta + e^{\alpha\beta cos\theta} \sum_{n=0}^{n} (-1)^n \epsilon_n \frac{I_n'(\alpha)}{I_n(\alpha)} I_n(\alpha\beta) cosn\theta \right]. \qquad [12]$$

The solution for the induced magnetic field is

$$B_{I,z}(r,\theta) = -\frac{R_m B_o G R^2}{8\alpha^2 \eta} \psi_2, \qquad [13]$$

where

$$\psi_2 = \left[e^{-\alpha\beta cos\theta} \sum_{n=0}^{\infty} \epsilon_n \frac{I_n'(\alpha)}{I_n(\alpha)} I_n(\alpha\beta) cosn\theta - e^{\alpha\beta cos\theta} \sum_{n=0}^{\infty} (-1)^n \epsilon_n \frac{I_n'(\alpha)}{I_n(\alpha)} I_n(\alpha\beta) cosn\theta - 2\beta cos(\theta) \right], \qquad [14]$$

and the I_n are modified Bessel functions, $R_m = 4\pi\sigma\mu R$ is the magnetic Reynold's number, $\alpha = \frac{H}{2}$, $\beta = \frac{r}{R}$, $\epsilon_0 = 1$, and $\epsilon_{n>0} = 2$. The solutions are functions of the Hartman number,

$$H = B_o R \sqrt{\frac{\sigma}{\eta}}, \qquad [15]$$

a dimensionless parameter characterizing the strength of the magnetohydrodynamic interaction. Figures 1 and 2 show plots of the dimensionless velocity profile, ψ_1, for Hartman numbers 0 and 4 and Figure 3 shows the induced magnetic field for Hartman number 4. The currents predicted by this solution follow the contour lines in Figure 3.

The maximum electric potential V across the tube is obtained by integrating the radial electric field:

$$V = 2S\mu B_o R v_o, \qquad [16]$$

where v_0 is the mean velocity in the tube and S is a dimensionless parameter. S varies from 1.00 to 0.95 as the Hartman number increases from 0 to 10. Eq. [16] is the well established electromagnetic flowmeter equation (7).

The flux of the fluid is obtained by integrating the velocity profile over the cross-section of the tube. The ratio of the fluid flux Q and the pressure gradient along the fluid G is characterized by the dimensionless parameter γ:

$$\gamma = (\frac{A^2}{\eta\pi})\frac{G}{Q}. \qquad [17]$$

The exact solution yields

$$\gamma_e = \frac{H}{\left[\frac{I_1^3(\alpha)}{I_0(\alpha)} - \sum_{n=0}^{\infty}(-1)^n \frac{I_{n-1}(\alpha)I_{n+1}(\alpha)}{I_n(\alpha)}(I_{n-1}(\alpha) + I_{n+1}(\alpha))\right]}. \qquad [18]$$

In the case of Poiseuille flow (no magnetic effect), $\gamma = 8$.

Approximate Solution

In 1973, Vardanyan presented an approximate laminar solution for the velocity profile of fluid flowing in a non-conducting, straight, circular tube with flow transverse to a magnetic field, assuming the magnetic fields induced in the fluid are negligible. The steady state Navier-Stokes equation in this approximation is

$$G = -\frac{H^2}{R^2}\mu^2\eta v_z + \eta \nabla^2 v_z, \qquad [19]$$

and the solution for the velocity profile is

$$v_z(r) = -\frac{GR}{\eta H^2\mu^2}\left(1 - \frac{I_0(H\beta)}{I_0(H)}\right). \qquad [20]$$

Other authors have obtained similar solutions (6). Vardanyan assumed that the induced magnetic fields are negligible because the magnetic Reynold's number for blood is small, but this assumption can not be made (8). In a non-conducting tube, the magnetohydrodynamic effect results from induced currents flowing in closed loops. By ignoring the induced magnetic fields, Vardanyan introduced a non-physical current,

$$\vec{j} = \mu\sigma(\vec{v} \times \vec{B}), \qquad [21]$$

which flows perpendicular to the direction of fluid flow and perpendicular to the applied magnetic field, without a return path. The approximate solution yields

$$\gamma_a = \left(\frac{H^2\mu^2 I_0(H)}{I_2(H)}\right). \qquad [22]$$

Further investigation reveals the inconsistency in this result. It can be shown that if the induced magnetic fields are not ignored, a cylindrically symmetric velocity profile has a nonzero force density due to the MHD effects, but that the total force is zero. The induced magnetic field must satisfy

$$\nabla^2 H_z = H_o R_m \left[\frac{sin\theta}{\beta}\frac{\partial v_z}{\partial\theta} - cos\theta\frac{\partial v_z}{\partial\beta}\right]. \qquad [23]$$

Using a cylindrical Green's function one may solve this equation for the H_z produced by a cylindrically symmetric velocity profile,

$$H_{z-symm}(r,\theta) = H_o R_m cos\theta f(\beta) \qquad [24]$$

where $f(\beta)$ is zero at $\beta = 1$. Substituting H_{z-symm} into the MHD force density and integrating over the cross section of the tube results in a zero total MHD retarding force. This result predicts that a cylindrically symmetric flow profile will experience no magnetohydrodynamic slowing, contradicting the prediction of Eq. [22].

Comparison with Data of Hartman and Lazarus

The classic experimental data for magnetohydrodynamic fluid flow in circular tubes was obtained by Hartman and Lazarus with mercury in 1937 (2). The exact and approximate solutions are compared in Fig. 4, where the parameters γ_e, γ_a, and the Hartman and Lazarus data are plotted. Both γ_e and γ_a approach the value expected for Poiseuille flow as the Hartman number goes to zero. It is apparent from Fig. 4 that γ_a rapidly diverges from γ_e and the mercury data. Gold shows that his solution is valid up to Hartman numbers around twenty, at which point the series in γ_e ceases to converge.

Experiments

Experiments to verify that the exact solution predicts the magnetohydrodynamic behavior of ionic fluids in magnetic fields in the range used for NMR were performed with 15 percent saline flowing in a 22 m length of 0.013 m I.D. flexible PVC tubing under constant pressure heads ranging from 0.002 to 0.08 m (Fig. 5). The density, viscosity, and conductivity of the saline were taken to be $\rho = 1106.51$ kg/m^3, $\eta = 1.354$ cp, and $\sigma = 17.1$ s/m respectively. The tubing had a 4.5 m straight section and a 17.5 meter section coiled into 30 loops each with a radius of curvature of 0.09 m. The pressure heads give rise to flows with Reynold's number, $R_e = 2\rho v R/\eta$, ranging from 250 to 950. Since flows with Reynold's numbers below 2000 are in the laminar range, it is appropriate to assume the fluid flow in this experiment is laminar.

Two magnets were used: a 2.35 Tesla superconducting magnet with 30 centimeter bore and a 4.70 Tesla superconducting magnet with 25 centimeter bore (with gradient and shim sets installed). The magnetic field applied to the fluid in the tube was changed from $\leq$0.01 to 2.35 or 4.70 Tesla by placing the coil of tubing 2 m away from the superconducting magnet and then placing the coil in the bore of the superconducting magnet. With the coil in the magnet, the fluid in the coiled tubing flowed transverse to the magnetic field and the fluid in the straight tubing flowed parallel to the magnetic field. Fluid flow parallel to the direction of the magnetic field does not produce an MHD effect. The Hartman numbers are 1.7 and 3.4 at 2.35 and 4.7 Tesla, respectively.

Outflow was collected in a graduated cylinder for periods of 2 to 10 minutes. Fluxes were calculated by dividing the volume collected by the sampling time. For each pressure head, the flux was measured repeatedly with a standard deviation of less than one percent, and the pressure heads were measured with an accuracy of one millimeter. Using the 2.35 Tesla magnet, the flow was reduced by less than one percent. The observed flow reductions using the 4.7 Tesla magnet are shown in Fig. 6.

The hydrodynamic equation of motion of the experimental apparatus needed to interpret the data is

$$\rho g h - \frac{\rho Q^2}{2A^2} = \delta P_{entrance} + G_{pois} L_{pois} + G_{curve} L_{curve}, \qquad [25]$$

where: $\delta P_{entrance}$ is the pressure drop on entering the tube,

$$\delta P_{entrance} = 1.19(\frac{\rho Q^2}{2A^2}); \qquad [26]$$

G_{pois} is the Poiseuille pressure gradient and L_{pois} is the length of the straight tube,

$$G_{pois} = \left(\frac{8\eta\pi}{A^2}\right) Q; \qquad [27]$$

and G_{curve} is the pressure gradient in the helical coil and L_{curve} is the length of the curved tube,

$$G_{curve} = \left(\frac{8\eta\pi}{A^2}\right) Q \frac{1}{1 - \left[1 - \left(\frac{5.3\eta A\sqrt{\frac{R_c}{R}}}{QR\rho}\right)^{.45}\right]^{2.222}}. \qquad [28]$$

R_c is the radius of curvature of the helix, h is the pressure head height, and A is the cross-sectional area of the tube. The entrance pressure drop and the curved pressure gradient are empirical relations (9). The theoretical predictions for hydrodynamic flow in the experimental apparatus are plotted in Fig. 6.

No solution for MHD flow in curved tubes currently exists. An approximate relation between flux and pressure head for the MHD case may be obtained by including the pressure drop due to MHD effects in a straight tube in the hydrodynamic equation:

$$\rho gh - \frac{\rho Q^2}{2A^2} = \delta P_{entrance} + G_{pois}\left[L_{pois} + (\gamma_e - 1)L_{curve}\right] + G_{curve}L_{curve}. \qquad [29]$$

This relation is plotted in Fig. 6. The predicted flow agrees well with the data at low fluxes, but it begins to diverge for flows larger than 0.3 l/min. This is attributed to secondary flows (10) which are expected to be similar to the induced currents produced in the MHD effect. These secondary flows may disturb the MHD induced currents and reduce the MHD effect in curved tubes. Fig. 6 also shows that the predictions based on the approximate solution do not agree with the experimental results.

Discussion and Conclusion

The exact solution can be used to predict an upper bound for the magnetohydrodynamic vascular pressure of a human in a 10 Tesla magnetic field. The predicted change between the total hydrodynamic vascular pressure and the total magnetohydrodynamic vascular pressure is less than 0.2 percent. The relative MHD pressure increase is independent of the velocity of the fluid, thus the fractional pressure increase is the same during systole and diastole. The theory of magnetohydrodynamic flow discussed above assumes steady laminar flow in a non-conducting tube. Large and small vascular conduits in the human body are generally laminar (11). In addition, the presence of a magnetic field tends to suppress turbulence and encourage laminar flow so that any parts of the circulation near turbulence are expected to move towards the laminar flow range. Vascular tissue is nearly six orders of magnitude more resistive than blood, thus it is a good approximation to treat the vascular conduits as non-conducting. Estimates of the upper bound on MHD pressure change in a typical human vasculature predicted by the exact solution are shown in Table 1, assuming a 10 Tesla magnetic field. The properties of the vasculature were obtained from tabulated data (12, 13). The hydrodynamic pressure drop through each section of the vascular system is calculated using Eq. [17] and $\gamma_p = 8$. The magnetohydrodynamic pressure drop is calculated using Eq. [17] and Eq. [18].

This estimate of the pressure increase is expected to be an upper bound because the estimate assumes that the magnetic field is everywhere perpendicular to the flow, that all of the conduits are straight, and that all of the flow is fully developed. Flow parallel to the magnetic field does not experience an increase in pressure. The predicted pressure increase in straight tubes is larger than the pressure increase observed in curved tubes. Flow in the aorta evolves from a cylindrically symmetric velocity profile which experiences no net retarding force into the asymmetric MHD velocity profile which experiences a net retarding force. The estimate ignores this evolution in the retarding force. This last point is particularly critical since it is in the aorta where the pressure change is most significant.

Calculations using Eq. [16] predict that at a peak flow of 10 l/min a 10 Tesla magnetic field will induce $\leq$ 100 mV MHD potentials across the aorta. The MHD induced potentials are large enough to be observed at the surface of the body and are comparable with the potentials associated with the ECG. An increase in the amplitude of the T- wave in the presence of a static magnetic field has been observed (14). The current density associated with these potentials is predicted to be $\leq$ 0.5 mA/cm^2 in the aorta. The effects of this current density on blood as well as the effect of the MHD electric fields upon surrounding tissue remains to be determined.

In summary, an exact solution for flow in a non-conducting, circular, straight tube has been applied to predict changes in pressure and electrical potential in the vasculature due to static magnetic fields. This solution was experimentally verified for flows of saline in fields of 2.35 and 4.7 Tesla. An approximate solution was demonstrated to produce incorrect results. Calculations based on the exact solution predict that a 10 Tesla magnetic field will have an insignificant effect on vascular pressure and will produce electrical potentials and current densities that are observable and whose biological significance remains to be determined.

Acknowledgement

Thanks is given to Dr. Li Han Chang for the use of the 4.7 Tesla magnet, to Dr. Stan Berger for his generous guidance, and to Dr. Richard Newmark and Blaise Frederick for their helpful assistance. This work was supported by the Director, Office of Energy Research, Research Medicine Radiation Biophysics Division, of the U.S. Department of Energy under Contract No. DE-AC03-76sf00098.

References

1. J. Hartman, *Mat.-fysiske Med.* **15**-6, 1(1937).

2. J. Hartman, F. Lazarus, *Mat.-fysiske Med.* **15**-7, 1(1937).

3. R. R. Gold, *J. Fluid Mech.* **13**, 511(1962).

4. V. A. Vardanyan, *Biofizika* **18**, 515(1973).

5. T.S. Tenforde, C.T. Gaffey, B.R. Moyer, T. F. Budinger, *Bioelectromagnetics* , 1(1982).

6. I. I. H. Chen, Subrata Saha, *J. Bioelectricity* **3**, 293(1984).

7. W. G. James, *Rev. Sci. Inst.* **22**, 989(1951).

8. J. E. Allen, *J. Appl. Phys.* **19**, 133(1986).

9. A. J. Ward-Smith, 'Internal Fluid Flow', Clarendon Press - Oxford, 221(1980).

10. S. A. Berger, L. Talbot, *Ann. Rev. Fluid Mech.* **15**, 461(1983).

11. B. Folkow, E. Neil, 'Circulation', Oxford University Press, 20(1971).

12. CRC, *Critical Reviews in Biomedical Engineering* **13**, 315.

13. R. M. Berne, M. N. Levy, 'Cardiovascular Physiology', The C. V. Mosby Co., 2(1986).

14. C. T. Gaffey, T. S. Tenforde, E. E. Dean, *Bioelectromagnetics* **1**, 209(1980).

Variables

H	=	uppercase h
α	=	lower case greek symbol alpha
v	=	lowercase vee
v_o	=	lowercase vee sub lowercase oh
Q	=	uppercase q
G	=	uppercase g
B	=	uppercase b
B_I	=	uppercase b sub uppercase i
B_o	=	uppercase b sub lowercase oh
E	=	uppercase e
η	=	lowercase greek symbol eta
σ	=	lowercase greek symbol sigma
β	=	lowercase greek symbol beta
ρ	=	lowercase greek symbol rho
π	=	lowercase greek symbol pi
γ	=	lowercase greek symbol gamma
γ_a	=	lowercase greek symbol gamma sub lowercase A
γ_e	=	lowercase greek symbol gamma sub lowercase E
$\delta P_{entrance}$	=	lowercase greek delta symbol uppercase p sub entrance

Variables - continued

R = uppercase r

A = uppercase a

Rc = uppercase R sub lowercase C

h = lowercase H

r = lowercase R

z = lowercase Z

θ = lowercase greek symbol theta

I_n = uppercase i sub lowercase N

ϵ_n = lowercase greek symbol epsilon sub lowercase N

R_e = uppercase r sub lowercase E

R_m = uppercase r sub lowercase M

j = lowercase J

μ = lowercase greek symbol mu

n = lowercase N

ψ = lowercase greek symbol psi

V = uppercase v

S = uppercase s

G_{pois} = uppercase g sub pois

L_{pois} = uppercase L sub pois

G_{curve} = uppercase g sub curve

L_{curve} = uppercase L sub curve

Figure Captions

Figure 1 Dimensionless plot of the velocity profile for H = 0. Eq. [12] is plotted by equally spaced contour lines ranging from 0.00 at the perimeter to -1.00 at the center of the plot.

Figure 2 Dimensionless plot of the velocity profile for H = 4. Eq. [12] is plotted by equally spaced contour lines ranging from 0.00 at the perimeter to -0.70 at the center of the plot.

Figure 3 Dimensionless plot of the induced magnetic field for H = 4. Eq. [14] is plotted by equally spaced contour lines ranging from 0 at the perimeter to -0.12 at the center of each lobe.

Figure 4 Theoretical predictions for $\gamma = \frac{A^2}{\pi\eta}\frac{G}{Q}$ as a function of the Hartman number compared with the mercury data of Hartman and Lazarus. The solid line is the exact solution, the dotted line is the approximate solution, the dashed line is Poiseuille flow, and the circles are the Hartman and Lazarus data.

Figure 5 Diagram of the experimental apparatus for measuring decrease in flow in the presence of a magnetic field.

Figure 6 The flux of 15 percent NaCl versus pressure head height. The dotted line is the theoretical flow with no magnetic field, the solid line is the theoretical flow in a 4.7 Tesla magnetic field using the exact solution, the dashed line is the theoretical flow in a 4.7 Tesla magnetic field using the approximate solution. The asterisks are the experimental data in no magnetic field and the solid dots are the experimental data in a 4.7 Tesla magnetic field. The error bars are smaller than the dots used to plot the points.

Table Captions

Table 1 This table shows the maximum vascular pressure increase resulting from the MHD effect. R, L, and N are the radius, length, and number of the conduits. H is the Hartman number. ΔHDP is the hydrostatic pressure drop and ΔMHDP is the magnetohydrodynamic pressure drop through the conduit. The viscosity of blood is assumed to be 4.5 cp and the conductivity is assumed to be 0.6 s/m.

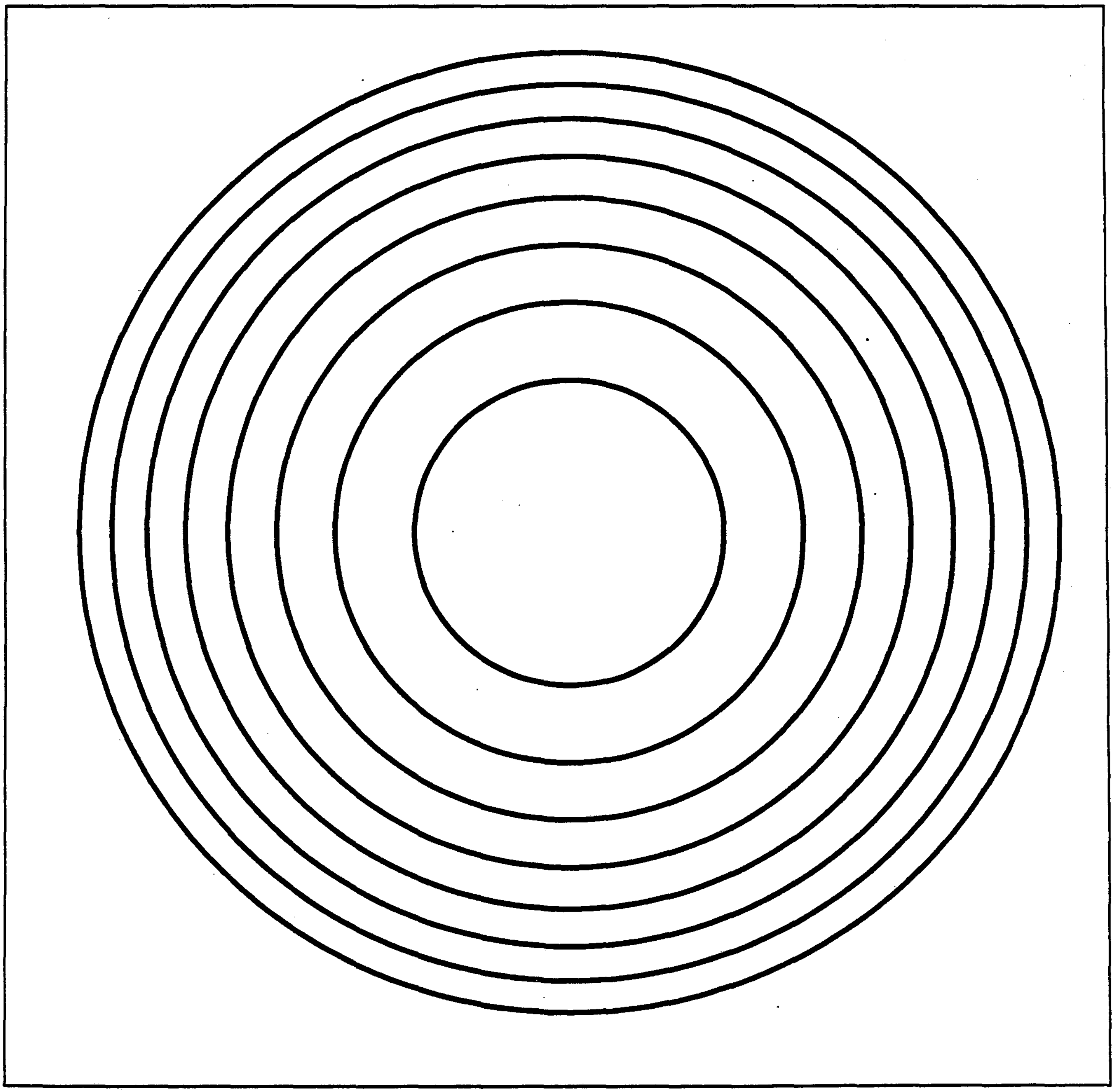

Figure 1

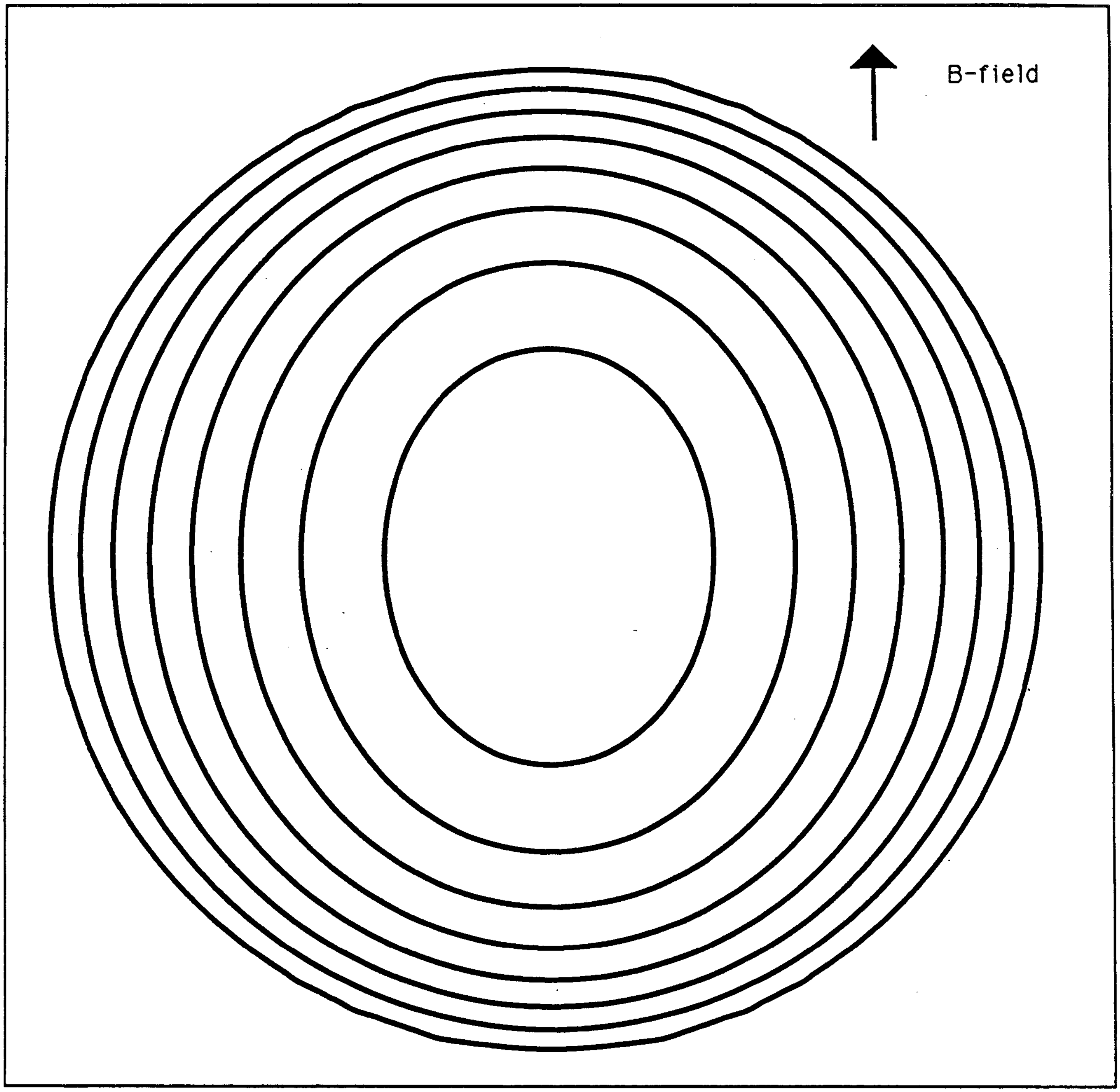

Figure 2

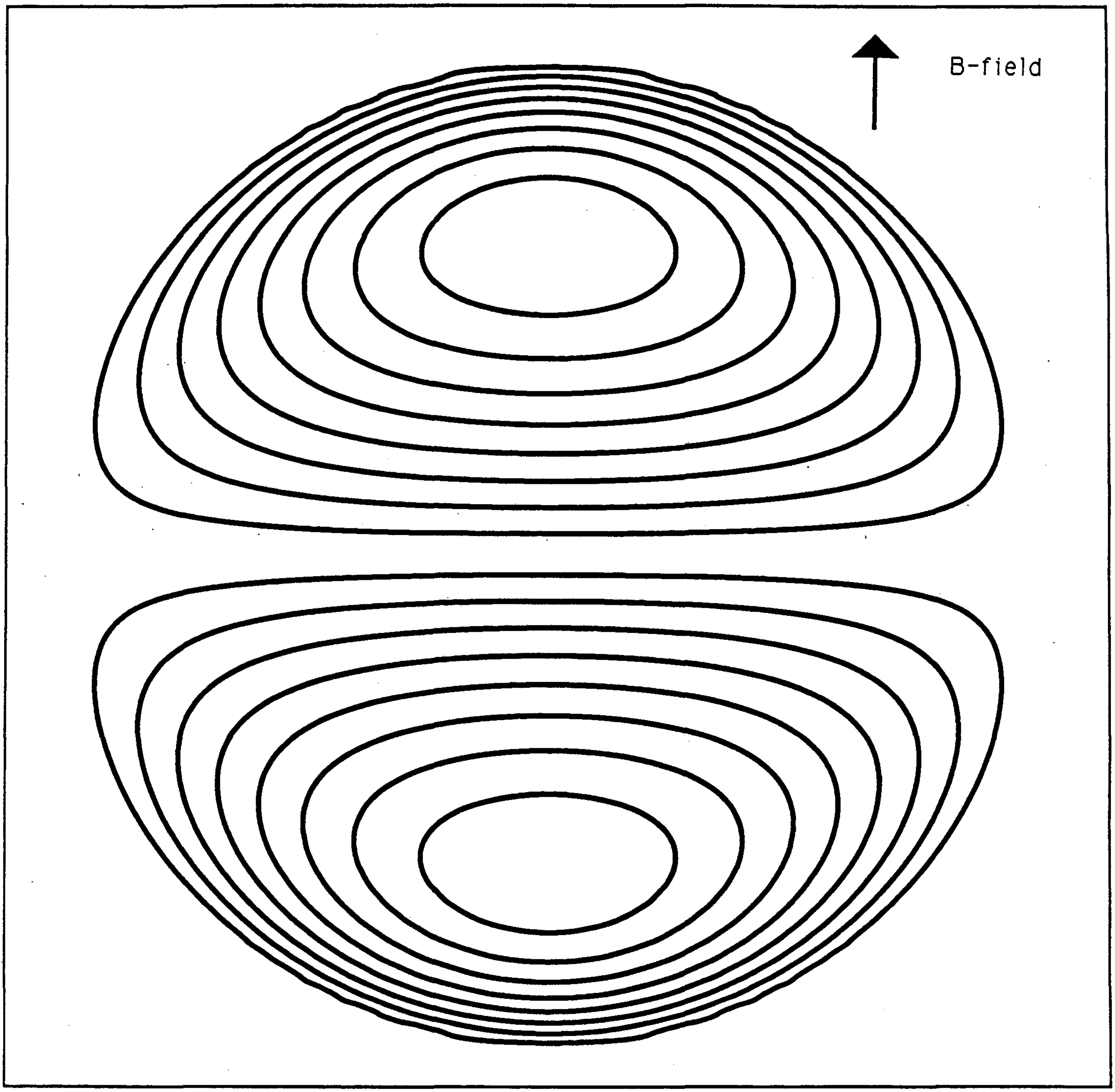

Figure 3

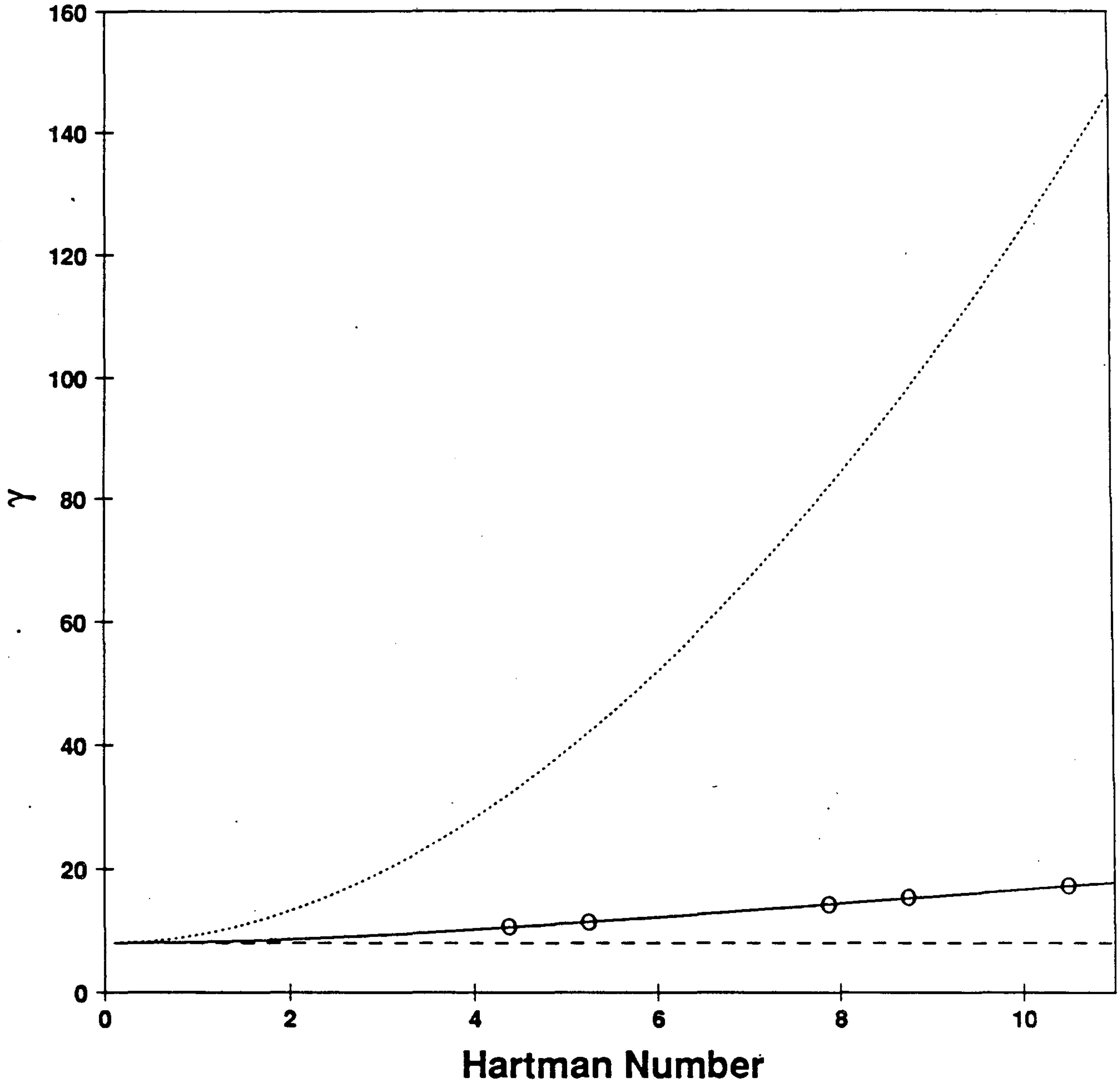

Figure 4

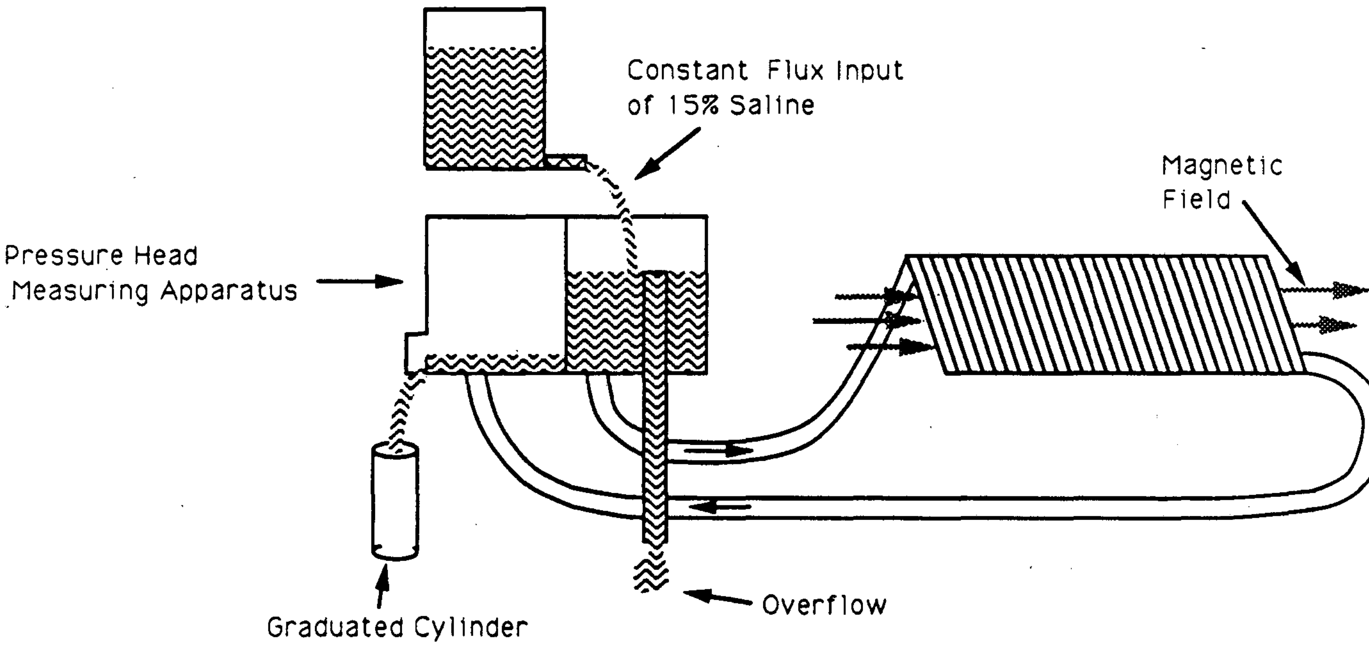
Constant Flux Input
of 15% Saline
Magnetic
Field
Pressure Head
Measuring Apparatus
Graduated Cylinder
Overflow

Figure 5

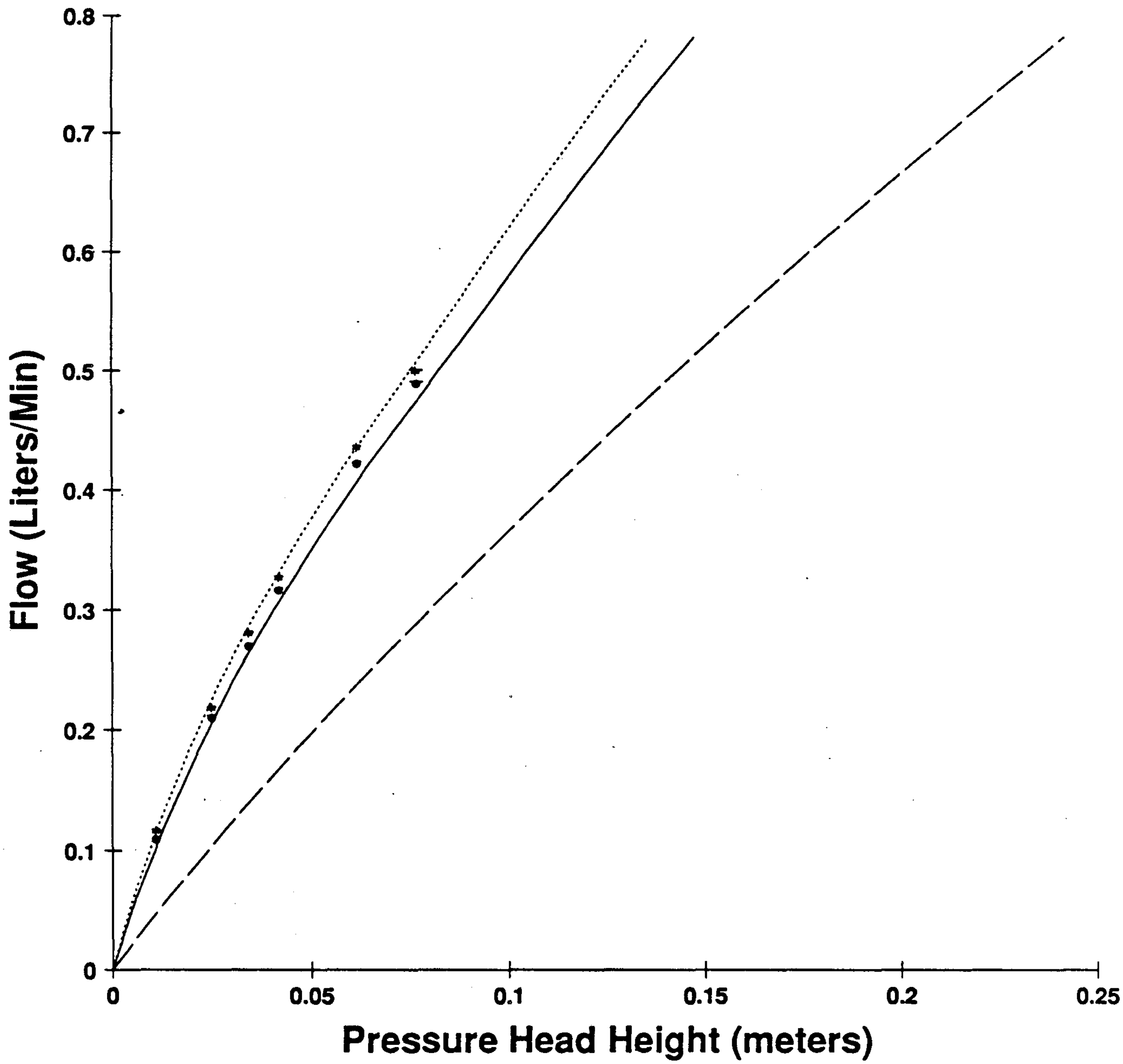

0.8
0.7
0.6
0.5
0.4
0.3
0.2
0.1
0
Flow (Liters/Min)
0
0.05
0.1
0.15
0.2
0.25
Pressure Head Height (meters)

Figure 6

Part of Vasculature	R(cm)	H	$\frac{\gamma_e}{\gamma_p}$	L(cm)	N	Δ HDP(torr)	ΔMHDP(torr)
Aorta	1.30	1.50	1.05	40	1	0.28	0.30
Large Arteries	0.20	0.23	1.00	20	20	12.10	12.12
Main Arteries	0.07	0.08	1.00	10	260	36.04	36.04
Secondary Arteries	0.06	0.06	1.00	0.4	800	1.06	1.06
Large Veins	0.14	0.16	1.00	10	600	0.80	0.80
Main Veins	0.35	0.40	1.00	20	40	0.66	0.66
Vena Cava	1.50	1.73	1.06	45	1	0.18	0.18

Table 1